

# Methanol oxidation to formaldehyde on VSiBEA zeolite

**Citation for published version (APA):**

Tranca, D. C., Keil, F. J., Tranca, I. C., Calatayud, M., Dzwigaj, S., Trejda, M., & Tielens, F. (2015). Methanol oxidation to formaldehyde on VSiBEA zeolite: a combined DFT/vdW/transition path sampling and experimental study. *Journal of Physical Chemistry C*, 119(24), 13619–13631. <https://doi.org/10.1021/acs.jpcc.5b01911>

**Document license:**  
TAVERNE

**DOI:**  
[10.1021/acs.jpcc.5b01911](https://doi.org/10.1021/acs.jpcc.5b01911)

**Document status and date:**  
Published: 11/05/2015

**Document Version:**  
Publisher's PDF, also known as Version of Record (includes final page, issue and volume numbers)

**Please check the document version of this publication:**

- A submitted manuscript is the version of the article upon submission and before peer-review. There can be important differences between the submitted version and the official published version of record. People interested in the research are advised to contact the author for the final version of the publication, or visit the DOI to the publisher's website.
- The final author version and the galley proof are versions of the publication after peer review.
- The final published version features the final layout of the paper including the volume, issue and page numbers.

[Link to publication](#)

**General rights**

Copyright and moral rights for the publications made accessible in the public portal are retained by the authors and/or other copyright owners and it is a condition of accessing publications that users recognise and abide by the legal requirements associated with these rights.

- Users may download and print one copy of any publication from the public portal for the purpose of private study or research.
- You may not further distribute the material or use it for any profit-making activity or commercial gain
- You may freely distribute the URL identifying the publication in the public portal.

If the publication is distributed under the terms of Article 25fa of the Dutch Copyright Act, indicated by the "Taverne" license above, please follow below link for the End User Agreement:

[www.tue.nl/taverne](http://www.tue.nl/taverne)

**Take down policy**

If you believe that this document breaches copyright please contact us at:

[openaccess@tue.nl](mailto:openaccess@tue.nl)

providing details and we will investigate your claim.

# Methanol Oxidation to Formaldehyde on VSiBEA Zeolite: A Combined DFT/vdW/Transition Path Sampling and Experimental Study

Diana C. Tranca,<sup>\*,†,‡</sup> Frerich J. Keil,<sup>\*,†</sup> Ionut Tranca,<sup>§</sup> Monica Calatayud,<sup>||,⊥</sup> Stanislaw Dzwigaj,<sup>\*,‡</sup> Maciej Trejda,<sup>#</sup> and Frederik Tielens<sup>‡,⊗</sup>

<sup>†</sup>Technische Universität Hamburg Harburg, Chemische Reaktionstechnik, Eißendorfer Straße 38, 21073 Hamburg, Germany

<sup>‡</sup>Sorbonne Université, UPMC, CNRS, UMR 7197, Laboratoire de Réactivité de Surface, Université Pierre et Marie Curie - Paris 6, Site d'Ivry - Le Raphaël, 3 Rue Galilée, 94200 Ivry-Sur-Seine, France

<sup>§</sup>Laboratory of Inorganic Materials Chemistry, Schuit Institute of Catalysis, Eindhoven University of Technology, Den Dolech 2, 5612 AZ, Eindhoven, The Netherlands

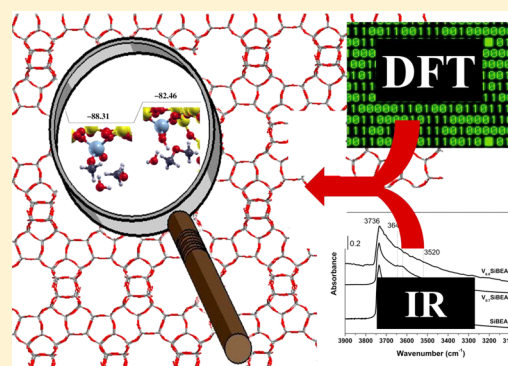
<sup>||</sup>UPMC Univ Paris 06, UMR 7616, Laboratoire de Chimie Théorique, F-75005, Paris, France

<sup>#</sup>Adam Mickiewicz University, Faculty of Chemistry, Grunwaldzka 6, PL-60-780 Poznan, Poland

<sup>⊗</sup>Sorbonne Université, UPMC Univ Paris 06, UMR 7574, Laboratoire Chimie de la Matière Condensée, Collège de France, 11 Place Marcelin Berthelot, 75231 Paris Cedex 05, France

## S Supporting Information

**ABSTRACT:** Density functional calculations have been performed applying periodic boundary conditions to investigate the oxidation of methanol on vanadium-containing SiBEA zeolite (VSiBEA). Different types of reaction configurations have been set up in conformity with the experimental conditions. Thermodynamic property calculations for  $T > 0$  K have been performed and compared with the available experimental results. Transition path sampling was employed to unravel the reaction mechanisms for oxidation of methanol on vanadium-containing SiBEA zeolites at three temperatures (300, 415, and 523 K). Dispersion interactions were accounted for by adding a damped dispersion term to the PBE energies. The study of different reaction pathways was combined with experimental data that enabled us to shed more light on the reaction mechanism.



## INTRODUCTION

Zeolitic materials are extensively employed in petroleum refining, petrochemicals production, and pollution control, as well as catalysts in various reactions, such as alkylation, aromatization, and isomerization of hydrocarbons.<sup>1–8</sup> They can exhibit both Brønsted and Lewis acidic properties.<sup>9–11</sup>

For understanding the catalytic reactions at the molecular level, quantum chemical calculations based on density functional theory (DFT) combined with statistical thermodynamics and transition state theory have been employed successfully over the past few years.<sup>12–14</sup> Recently, different theoretical<sup>1,15–22,87–90</sup> and experimental results<sup>20,23</sup> on the vanadium framework sites in zeolites have been reported. It was shown that the isomorphous substitution of framework atoms in molecular sieve materials gives the possibility to modify their acidic and/or redox catalytic properties.<sup>1</sup> The isomorphous substitution of zeolite framework atoms by certain transition metals such as Ti or V creates redox catalysts with efficient activity for the partial oxidation of hydrocarbons and alcohols, epoxydation of olefins, hydroxylation of aromatics, or the ammoxidation of ketones.<sup>24</sup> These transition metal-substituted

zeolites or zeotypes have opened new ways for many applications, not only in petrochemical industry but also in various photochemical processes, such as decomposition of NO, reduction of CO<sub>2</sub> with H<sub>2</sub>O, or the reduction of N<sub>2</sub>O with CO. Incorporation of vanadium in the framework T-atom sites of zeolite BEA is strongly favored when the zeolite is previously dealuminated by treatment with nitric acid solution.<sup>1</sup> The vanadium incorporation results from the reaction between the mononuclear cationic V species of the precursor solution and the silanol groups created by dealumination. The vanadium framework sites have been characterized by their calculated geometric parameters, vibrational frequencies, and deprotonation energies.<sup>1</sup> Vanadium is stabilized in the zeolite framework sites, forming a very stable pseudo-tetrahedral V(V) species with a vanadyl group.<sup>1</sup> In addition to this stable structure, a whole series of activated, less stable sites can exist and may be

Received: February 26, 2015

Revised: May 11, 2015

Published: May 11, 2015

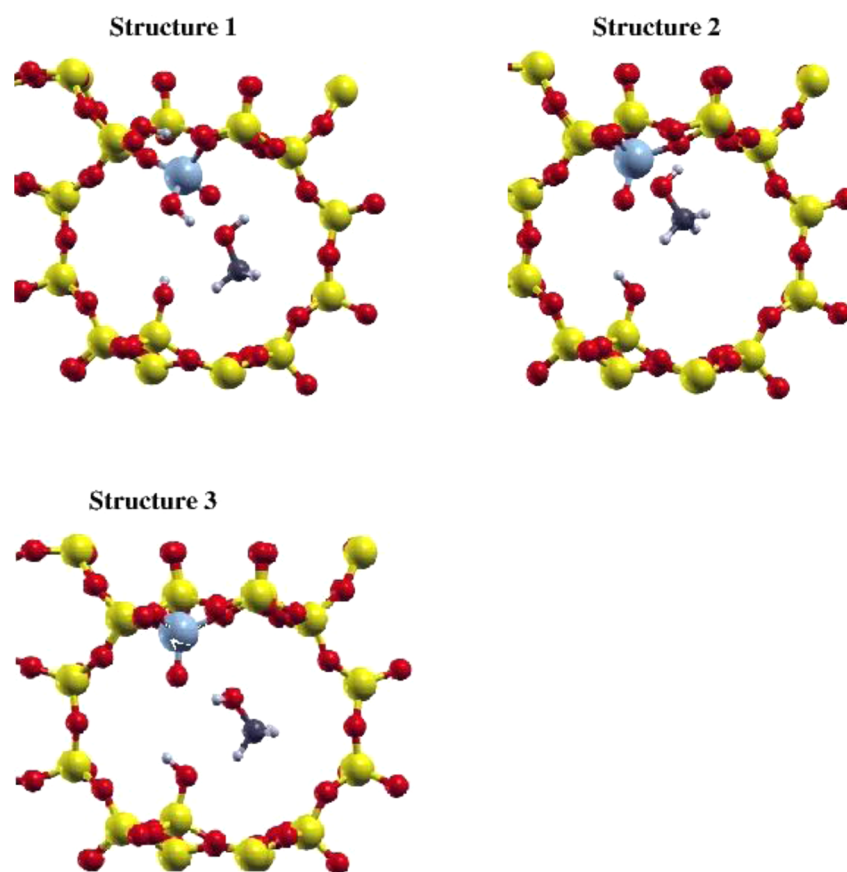


**Figure 1.** Methanol adsorbed on VBEA zeolite. Three different types of reactant structures are shown for the adsorption of methanol on VBEA zeolite. Structure 1 corresponds to eq 2; Structure 2 is similar to the Sauer model and corresponds to eq 1; Structure 3 corresponds to eq 1, too. The difference between Structure 2 and Structure 3 is the position and orientation of the methanol molecule: pointing toward the V–OSi group in the first case and toward the V=O bond in the second case (color code: carbon, dark gray; hydrogen, light gray; oxygen, red; silicon, yellow; vanadium, cyan).

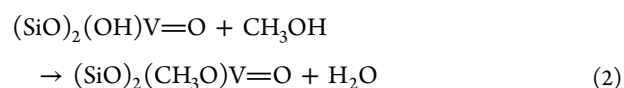
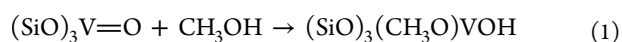
considered as the precursor of the catalytic properties of vanadium SiBEA zeolite (VSiBEA).

Chemical reactions involving methanol are important in many fields, e.g., fuel cells, catalysis, biological processes.<sup>13,25,26</sup> One major application of methanol is the production of formaldehyde. About 40% of the existing methanol is converted into formaldehyde and further into products such as plastics, paints, and explosives.

Although there are known ways to obtain formaldehyde from methanol (dehydrogenation or oxidative dehydrogenation of methanol on Ag/Cu/MoO catalysts), these processes have two significant drawbacks: high operating temperatures (573–923 K) and the formation of several by-products such as carbon monoxide, carbon dioxide, dimethyl ether, methyl formate, and formic acid.<sup>27</sup> Because of these there is an ongoing research to develop improved ways for the conversion of methanol to formaldehyde.<sup>28,29</sup>

A recently investigated pathway is the oxidation of methanol on the V-BEA zeolite. While experimentally proven successfully,<sup>23</sup> the actual steps of this procedure are not fully understood. How does methanol actually adsorb on the V-BEA? Which is the reaction sequence for its oxidation?

On the basis of the experiments, two different model reactions at 523 K have been proposed:<sup>23</sup>



In eq 1, the vanadium center in V-BEA zeolite is assumed to be non-hydroxylated (i.e., the V atom is single bonded to 3 SiO groups and double bonded to an O atom, see structure V5 in refs 1 and 2). The reaction describes the breaking of the methanol O–H bond and the change of the V=O to V–O–H. The transformation of the CH<sub>3</sub>O into CH<sub>2</sub>O is not considered here. In eq 2, the vanadium center in the V-BEA zeolite is assumed to be hydroxylated (i.e., one of the SiO groups connected to the V atom is replaced by an OH group, see structure BVT5 or TV5 in refs 1 and 2). The reaction supposes that the hydroxyl hydrogen of the methanol group will interact now with the hydroxyl group of V–OH, forming water as a by-product.

Most computational studies address the electronic structure and bonding properties of clean vanadium oxide surfaces and supported vanadium oxide clusters,<sup>33–39</sup> with very few theoretical works dealing with the structure or reactivity of vanadium oxides under hydration conditions.<sup>40,41</sup>

On the basis of *ab initio* calculations, using an 8-atom V-BEA cluster, Romanyshyn et al.<sup>30,31</sup> have proposed the following model: in a first step the interaction of methanol with the non-hydroxylated V-BEA takes place at the level of the V–O–Si. This results in the formation of the H–OSi group as a stable by-product. In the second stage, the oxidation of the adsorbed

methanol to formaldehyde occurs. A different theoretical model has been proposed by Calatayud et al.<sup>25,26</sup> studying the oxidation of methanol on a V-supported Ti oxide cluster. The methanol oxidation takes place if (1) methanol points toward the V–OTi site or (2) methanol points toward the V=O site.

In the present article, both thermodynamic property calculations for methanol on VSiBEA and transition path sampling (TPS) simulations for observing how the process of oxidation takes place in detail are presented. The TPS simulations have been performed at temperatures close to the experimental ones. Large periodic structures have been considered. Both the hydroxylated and the non-hydroxylated cases were treated.

In a set of experiments, the partial oxidation of methanol to formaldehyde has been studied on VO<sub>x</sub>/CeO<sub>2</sub>/SiO<sub>2</sub>.<sup>32</sup> The effect of ceria was suggested to be a possible lowering of the reaction temperature down to 415 K. These experiments indicate that the ceria layer, to which the vanadate species are bound, participates in the formation of the products.<sup>32</sup> In the case of our system, we will show that the formation of formaldehyde can occur directly on VSiBEA at 415 K (see Figure 1, Structure 2).

This work aims to describe the oxidation mechanism of methanol to formaldehyde on VSiBEA by combining experimental and theoretical investigations. The experimental investigations allowed determining the acidic properties of VSiBEA zeolites and the nature and environment of V species. Both non-hydroxylated (SiO)<sub>3</sub>V=O and hydroxylated (SiO)<sub>2</sub>(HO)V=O vanadium species have been identified by experimental investigation and considered in the theoretical investigation of the mechanism of methanol oxidation. The basic vanadyl oxygen of hydroxylated (SiO)<sub>2</sub>(HO)V=O species is proposed as an active site responsible for selective oxidation of methanol into formaldehyde on the VSiBEA zeolite. The experimental investigations of the methanol oxidation are in line with the theoretical investigations presented in this work.

First-principles calculations within the density functional theory framework applying periodic boundary conditions have been performed. Dispersion interactions were accounted for by adding a damped dispersion term to the PBE energies. From intrinsic energy barriers, intrinsic rate coefficients were calculated by means of transition state theory. Transition path sampling (TPS) was employed to unravel the reaction mechanism for the oxidation of methanol. Thermodynamic properties (adsorption enthalpies, entropies, free energies) were calculated for temperatures used in the experiments.

## ■ COMPUTATIONAL DETAILS

**A. DFT Calculations Applying Periodic Boundary Conditions.** The DFT calculations were carried out using the VASP program (Vienna Ab Initio Simulation Package),<sup>42–45</sup> where the electronic wave functions have been expanded into plane waves up to an energy cutoff of 500 eV, and a projected-augmented-wave (PAW)<sup>46</sup> scheme has been used in order to describe the interactions between the valence electrons and the nuclei (ions).

Thermodynamic properties have been calculated in the framework of harmonic oscillator rigid rotator approximation. For details see ref 13.

The crystal structure of VSiBEA consists of a tetragonal unit cell with fixed edge lengths of  $a = 12.70 \text{ \AA}$ ,  $b = 12.70 \text{ \AA}$ ,  $c = 26.77 \text{ \AA}$ . According to the crystallographic data,<sup>47</sup> the beta

zeolite contains nine different tetrahedral sites (T-sites).<sup>48</sup> The most stable site for V incorporation was proven to be the T1 site.<sup>48</sup> Therefore, the reaction calculations performed in this article were done for this site. During the simulations all the atoms were allowed to relax. This means >200 atoms in the non-hydroxylated or hydroxylated unit cell structures.

The transition states were localized by using the improved dimer method.<sup>49</sup> Convergence was considered to be achieved when the forces were below 0.01 eV/Å. Stationary points found were characterized by harmonic frequencies obtained by diagonalization of the full dynamical matrices. The force constants were obtained by numerical differentiation of forces with a step size of 0.02 Å.

Open shell calculations have been performed for all the transition states and product calculations, in order to allow for a variable oxidation state of vanadium. In order to compute the adsorption energies, the total energies for the vacuum molecules (methanol, formaldehyde, etc.) had to be computed. This has been done by considering each of these molecules isolated in a large  $25 \times 25 \times 25 \text{ \AA}^3$  unit cell.

Adsorption energy at  $T = 0 \text{ K}$  was calculated from the PBE energies as

$$\Delta E_{\text{ads}}^{T=0} = E_{\text{system}} - (E_{\text{molecule}} + E_{\text{zeolite}}) \quad (3)$$

Zero point corrected vibrational adsorption energies were obtained from

$$\Delta E_{\text{ads},0}^{T=0} = \Delta E_{\text{ads}}^{T=0} + \sum_{ip}^{\text{modes}} \frac{1}{2} h\omega_{ip} - \sum_{is}^{\text{modes}} \frac{1}{2} h\omega_{is} - \sum_{iA}^{\text{modes}} \frac{1}{2} h\omega_{iA} \quad (4)$$

where  $\sum_{ip}^{\text{modes}} 1/2 h\omega_{ip}$  is the contribution of the vibrational frequencies associated with the adsorbed system,  $\sum_{is}^{\text{modes}} 1/2 h\omega_{is}$  are the vibrational frequencies corresponding to the zeolite, and  $\sum_{iA}^{\text{modes}} 1/2 h\omega_{iA}$  are the vibrational frequencies corresponding to the gas phase molecule.

**B. Dispersion Corrections.** van der Waals (VdW) interactions between atoms and molecules caused by long-range electron correlation contribute significantly to the heat of adsorption.<sup>50,51</sup> However, the functionals which can be used efficiently in periodic solid-state simulations do not properly account for long-range dispersion interactions<sup>52,53</sup> and are subject to the self-interaction error.<sup>54–57</sup> Many of the computational approaches that can be used to describe dispersion interactions such as the treatment of dynamic correlations within the random phase approximation (RPA) theorem,<sup>58,59</sup> the Langreth method,<sup>60</sup> or MP2 calculations are very time-consuming for extended systems such as zeolites. A computationally less demanding approach consists in adding a pairwise interatomic  $C_6 R^{-6}$  term to the DFT energy.<sup>60–69</sup> Here the semiempirical approach of Grimme is adopted.<sup>61–64</sup> The total energy can be written as

$$E_{\text{TOTAL}} = E_{\text{PBE}} + E_{\text{DISP}} \quad (5)$$

where  $E_{\text{PBE}}$  is the electronic energy and  $E_{\text{DISP}}$  is the empirical dispersion correction term D3-BJ.<sup>64</sup> The Grimme approach has been applied to a variety of molecules in diverse sets of host structures, including several studies of zeolites<sup>12,13,70–74</sup> providing enough evidence that this semiempirical approach can be used successfully to estimate interaction energies.

**C. Transition Path Sampling.** There are several methods available for obtaining reaction pathways. The traditional approach has been finding transition states, or local saddle points, and then follow the imaginary mode to find the reactants and the products associated with the transition state.<sup>75</sup> A more effective approach would involve sampling various dynamic pathways that are representative of the true reaction process.<sup>75</sup> The transition path sampling (TPS) is such an approach.<sup>76–83</sup> Path finding algorithms, including the recently developed transition-path theory (TPT), have been reviewed by Weinan and Vanden-Eijnden.<sup>84</sup>

The TPS method is based on a random walk in the space of reactive trajectories. The reactive trajectory is an equilibrium object defined as an ordered sequence of states (i.e., atomic positions and corresponding momenta) connecting reactants and products. They are generated by Molecular Dynamics (MD) simulations. Similar to Monte Carlo (MC) simulations, a random walk in reactive trajectory space is executed by means of trial moves, called “shooting” and “shifting”. In a shooting move, a certain state on the previous trajectory is selected randomly and the corresponding momenta are modified by adding a small Boltzmann distributed noise to the respective previous values. The equations of motion are integrated forward and backward in time. If the new trajectory still connects the reactants and products, it is accepted, otherwise it is rejected. In a “shifting” move a state close to the reactant or product region is chosen. Thus, all states before or after, respectively, on the trajectory are removed and the same number of states is added to the other end of trajectory by integration of the equation of motion. The TPS has been implemented as described in ref 83. The initial trajectory has been obtained by forward and backward integration of the equations of motion starting from a configuration close to the transition state and randomly generated momenta. The simulations were performed in the canonical ensemble. The MD time steps were set to 1 fs. About 1500 trajectories have been calculated. The electronic energies were taken from the VASP code at each time step.

The transition states (TS) have been found using the dimer method<sup>49</sup> as implemented in the VASP program. Starting from the transition state (TS), the reactants and products are determined employing the transition path sampling (TPS) approach. The reaction pathway has been determined at three temperatures: 300, 415, and 523 K.

The frequency analysis revealed the presence of exactly one imaginary frequency for all transition states. Visualization of the normal modes corresponding to the imaginary frequencies was used to confirm that they indeed correspond to the expected motion of atoms.

## ■ EXPERIMENTAL DETAILS

**A. Materials.** A tetraethylammonium BEA zeolite (TEA-BEA) (Si/Al = 11) provided by RIPP (China) was treated with a 13 N HNO<sub>3</sub> solution (4 h, 353 K) under stirring to obtain a dealuminated BEA (Si/Al = 1000) noted SiBEA, which was separated by centrifugation, washed with distilled water and finally dried in air overnight at 353 K.

The SiBEA solid was then contacted with an aqueous solution of ammonium metavanadate (NH<sub>4</sub>VO<sub>3</sub>) in large excess (2 g of zeolite in 20 mL of solution). The concentration of NH<sub>4</sub>VO<sub>3</sub> solution was varied from 0.7 × 10<sup>-2</sup> to 19 × 10<sup>-2</sup> mol L<sup>-1</sup> in order to obtain samples with different vanadium contents because of its low concentration at pH = 2.5, the

initial aqueous solution is expected to contain mainly monomeric VO<sub>2</sub><sup>+</sup> ions.<sup>24</sup> The suspension was left for 3 days at room temperature without stirring. The solids with vanadium were recovered by centrifugation and dried at 353 K overnight. VSiBEA samples with 0.7 and 6 V wt % were labeled V<sub>0.7</sub>SiBEA and V<sub>6.0</sub>SiBEA, respectively.

**B. Experimental Techniques.** Infrared spectra were registered with a Bruker Vector 22 FTIR spectrometer. Samples were pressed at ~0.2 tons cm<sup>-2</sup> into thin wafers of ~10 mg cm<sup>-2</sup> and were placed inside the cell. Catalysts were outgassed at 673 K for 3 h and then contacted with pyridine (PY) at 423 K. After saturation with PY, the samples were degassed at 423, 473, 523, and 573 K under vacuum for 30 min at each temperature. Spectra were recorded at room temperature in the range from 400–4000 cm<sup>-1</sup>. The spectrum without any sample (“background spectrum”) was subtracted from all recorded spectra. The IR spectra of the activated samples (after evacuation at 673 K) were subtracted from those recorded after adsorption of PY followed by various treatments. Diffuse reflectance UV–vis (DR UV–vis) spectra were registered with a Cary 5E spectrometer equipped with an integrator and a double monochromator.

**C. Methanol Oxidation.** Methanol oxidation was performed in a fixed-bed flow reactor (diameter = 5 mm; length = 70 mm). An amount of 0.04 g of catalyst with grain size of 0.5 < diameter < 1 mm was placed into the reactor (4 mm height). The samples were activated in flowing argon (40 mL min<sup>-1</sup>) at 673 K for 2 h (heating rate of 15 K min<sup>-1</sup>). Then, the temperature was lowered to 523 K. The reactant mixture of Ar/O<sub>2</sub>/MeOH (88/8/4 mol %) was supplied at the rate of 40 mL min<sup>-1</sup>. Methanol (Chempur Poland) was fed into the flow reactor by bubbling argon gas through a glass saturator filled with methanol.

Methanol decomposition was performed in the same fixed-bed flow reactor under the same operating conditions. The reactor effluent was analyzed online by employing two gas chromatographs: the first (8000 Top) equipped with a capillary column of DB-1 operated at 313 K was used to analyze organic compounds with a flame ionization detector (FID) and the second, containing Porapak Q and 5A molecular sieves columns, to analyze O<sub>2</sub>, CO<sub>2</sub>, CO, H<sub>2</sub>O, and CH<sub>3</sub>OH with a TCD detector. For the latter, the columns were heated as follows: 5 min at 358 K, increase of temperature to 408 K (heating rate 5 K min<sup>-1</sup>), 4 min at 408 K, cooling down to 358 K (for the automatic injection on the column with molecular sieve 5A), 10 min at 358 K, increase of temperature to 408 K (heating rate 10 K min<sup>-1</sup>), 11 min at 408 K. Argon was the carrier gas. The outlet stream line from the reactor to the gas chromatograph was heated at about 373 K to avoid condensation of reaction products.

## ■ RESULTS AND DISCUSSION

**A. Description of the Theoretical Results: Reaction Pathways.** *Structure 1.* To study the reaction of methanol on the V-BEA zeolite, three different models were taken into consideration (see Figure 1), based on our earlier experimental results.<sup>23</sup> The first structure (Structure 1, Figure 1) corresponds to the situation described in eq 2. In this structure, vanadium is single-bonded to two O–Si groups as well as to a hydroxyl group and double-bonded to a vanadyl oxygen atom. The CH<sub>3</sub>OH molecule is in close vicinity to the vanadium atom (the distance between V–OH and the O belonging to CH<sub>3</sub>OH is 1.63 Å). For this structure an adsorption energy of –49.2

kJ/mol (see eq 3) (ZPE, zero point energy; corrected,  $-44.6$  kJ/mol; see eq 4) was found (Table 1).

**Table 1. Adsorption Energies at  $T = 0$  K for the Reactants<sup>a</sup>**

structure considered	$\Delta E_{\text{ads,DFT}+D}^{\text{OK}}$ (ZPE)
Structure 1	$-49.2$ ( $-44.6$ )
Structure 2	$-46.2$ ( $-40.3$ )
Structure 3	$-32.9$ ( $-29.7$ )

<sup>a</sup>All values are given in kJ/mol. In brackets ZPE (zero-point vibrational energies) corrected energies are shown.

From this reactant, a transition state (TS) associated with the formation of the V–OCH<sub>3</sub> group is identified (see Figure 2). Within this, the H atom belonging to the methanol group is in close proximity to the V–OH bond ( $d(\text{V–O(H)}\cdots\text{H}) = 1.18$  Å,  $d(\text{H}_3\text{CO}\cdots\text{H}) = 1.24$  Å). Such a TS favors the formation of water and of the methoxy (methoxide) group, in agreement with the experimental results of Trejda et al.<sup>19</sup> The TS has an activation energy of 75.6 kJ/mol (ZPE corrected 66.4 kJ/mol), see Table 3. The value of 66.4 kJ/mol for the TS shows that for this reaction path the formation of formaldehyde or of dimethyl ether (the other potential product) is plausible.

Along the reaction path, the methoxide and water intermediate state is a stable structure with the relative total energy of  $-38.1$  kJ/mol (see Figure 2). From this state on, in order to form the final product, one has to add a second methanol molecule inside the V-BEA cage. The added methanol interacts with the methoxide molecule leading to the formation of dimethyl ether and water.

Different snapshots from the MD simulations performed at  $T = 523$  K are shown in the Supporting Information (Figure 1). In these snapshots different intermediate states are shown until the final product is formed. The products are dimethyl ether and water. The adsorption energy of the final product (dimethyl ether + water) is  $-111.6$  kJ/mol.

For temperatures smaller than  $T = 523$  K (i.e.,  $T = 300$  K and  $T = 415$  K) the reaction mechanism ends with the formation of

the methoxide molecule. Dimethyl ether or formaldehyde molecules are not obtained at these temperatures.

**Structure 2.** The second and third structures (Figure 1: Structure 2 and Structure 3) correspond to eq 1. In Structure 2, vanadium is single-bonded to three O–Si groups and double bonded to an O atom. The H atom belonging to CH<sub>3</sub>OH points toward the V–O–Si group ( $d(\text{VO}\cdots\text{H}) = 1.22$  Å).

This system is similar to the one proposed by Sauer et al.<sup>85,86</sup> The adsorption energy for this structure is  $-46.2$  kJ/mol (ZPE corrected,  $-40.3$  kJ/mol) (Table 1). Systems like Structure 2 have been intensively investigated in other theoretical papers.<sup>19–22</sup> This structure has been adsorbed on various type of surfaces (VO<sub>x</sub>/SiO<sub>2</sub>, VO<sub>x</sub>/TiO<sub>2</sub>, VO<sub>x</sub>/ZrO<sub>2</sub>, [VO]<sup>1+</sup>-ZSM-5).<sup>19–22</sup> The values obtained for the adsorption energies of the methanol on these surfaces are between  $-32$  kJ/mol and  $-97$  kJ/mol.<sup>19–22</sup> This difference depends on a lot of factors like the size of the cluster and the composition of the surface/zeolite (type of the metal atoms). In the cluster calculations, the environment interactions are neglected. Depending on the cluster size the values obtained for the reaction mechanism can fluctuate. Other quantities that affect the final result are the functionals and the methods that are used. In our calculations we have a unit cell composed of approximately 200 atoms and we are dealing with periodic system calculations.

Because of the fact that the CH<sub>3</sub>OH molecule is placed in the close proximity of the vanadium site, in the first step of the reaction an interaction between the alcohol proton of CH<sub>3</sub>OH and the V–O–Si site is observed. This interaction leads to the formation of a methoxy group and silanol (see Figure 3).

The transition state (TS) for Structure 2 is associated with the formation of V–OCH<sub>3</sub> and H–OSi bonds. In this stationary point, the vanadium atom is 5-fold coordinated, with a V–OCH<sub>3</sub> bond distance of 1.97 Å. The H–OSi distance is 1.22 Å. The energy barrier for this process is 69.3 (56.9) kJ/mol, see Table 3. The transition path sampling calculations done for this structure revealed that at both temperatures,  $T = 415$  K and  $T = 523$  K, the product formation can be observed (Supporting Information, Figure 2). The intermediates are the methoxy group and a silanol group with an energy of 23.9

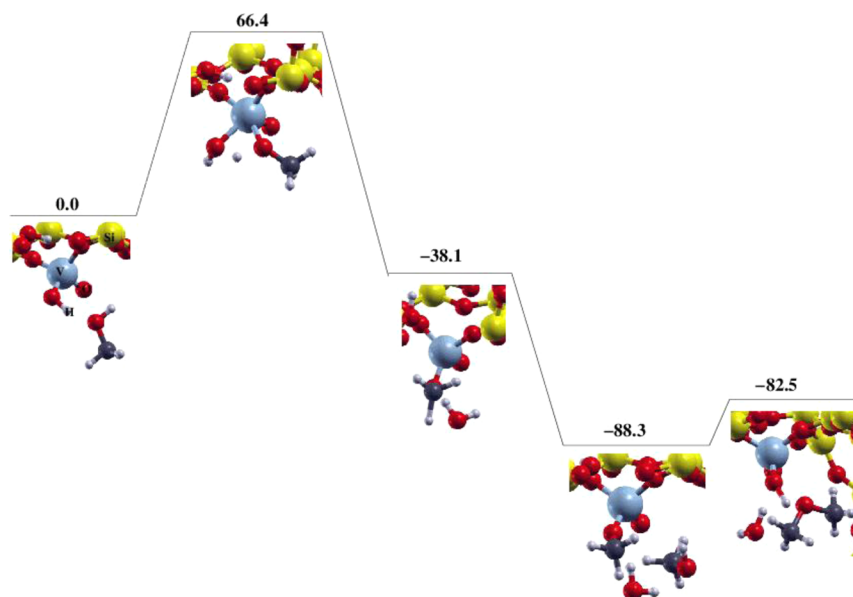


**Figure 2.** Reaction path diagram for Structure 1. The energies for the reactant, intermediate states, and the product are given in kJ/mol.

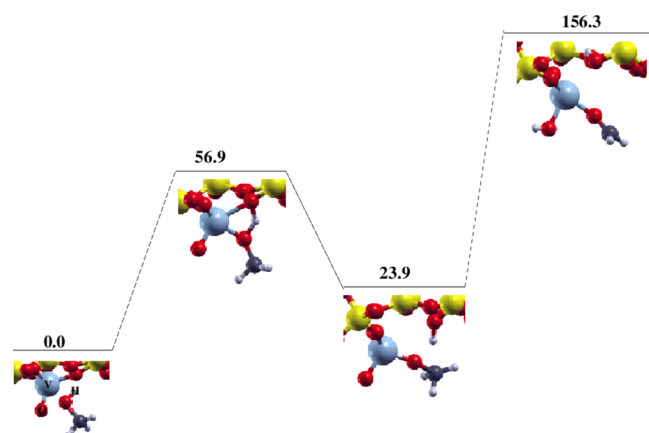


**Figure 3.** Reaction path diagram for Structure 2. The energies for the reactant, intermediate states, and the product are given in kJ/mol.

kJ/mol (see Figure 3). Further, the interaction between the methoxy group and the vanadium site leads to the formation of formaldehyde as final product. The adsorption energy of the formaldehyde product is  $-133.7$  kJ/mol.

To complete the catalytic cycle a further methanol molecule should be introduced into the system. The H atom belonging to the methanol will interact with the V–OH group leading to the formation of water and  $\text{OCH}_3$ .

The methoxy group will interact with the  $\text{VO}-\text{CH}_2$  leading to the formation of the  $\text{CH}_2-\text{O}-\text{CH}_3$  intermediate state. For forming the dimethyl ether, the intermediate  $\text{CH}_2-\text{O}-\text{CH}_3$  should be in close proximity of the Si–OH group. Once the proton is transferred from the Si–OH to the  $\text{CH}_2-\text{O}-\text{CH}_3$ , the second product ( $\text{CH}_3-\text{O}-\text{CH}_3$ ) will be formed. Therefore, the reaction mechanism takes place in two steps:

- (1) Formation of the formaldehyde product.
- (2) Formation of water and dimethyl ether. After the formation of the dimethyl ether, the catalytic process is complete, meaning that the vanadium is bonded again via three SiO single bonds and one oxygen double bond.

**Structure 3.** Similar to Structure 2, the vanadium atom in Structure 3 is single-bonded to three O–Si groups and double-bonded to an O atom. However, the H atom belonging to the OH group of  $\text{CH}_3\text{OH}$  points toward the  $\text{V}=\text{O}$  bond (see Figure 1, Structure 3). The adsorption energy for methanol in this configuration was found to be smaller than in Structure 2, having the value of  $-32.9$  ( $-29.7$ ) kJ/mol (Table 1).

The transition state occurs when the H atom of the methanol comes into close proximity to the  $\text{V}=\text{O}$  bond (Figure 4). The proton is then transferred to  $\text{V}=\text{O}$ , forming V–OH and at the same time the methoxide structure (Figure 4).

For Structure 3, the obtained energy barrier is higher than the one for Structure 2, having a value of  $105.1$  ( $92.4$ ) kJ/mol (Table 3). This is because the cleavage of the  $\text{V}=\text{O}$  bond and the formation of V–OH and V– $\text{OCH}_3$  groups is more expensive than the cleavage of the V–OH bond from Structure 2. The fact that the proton is transferred to the vanadyl group destabilizes this structure compared to the TS for Structure 2 and makes the mechanism along Structure 2 more probable to happen. For the TS in Structure 3, the distance of V– $\text{OCH}_3$  is  $2.05$  Å and the distance for V–OH is  $1.15$  Å. After the transfer of the proton to the zeolite, the methoxide structure is formed (Figure 4c). For the methoxide structure, the distance V– $\text{OCH}_3$  is  $1.81$  Å,  $d(\text{V}-\text{OH}) = 1.92$  Å and  $d(\text{VO}-\text{H}) = 1.0$  Å. The relative total energy of this intermediate state with respect to the reactant state is  $43.4$  kJ/mol.

For forming the first final product, one of the hydrogen atoms belonging to  $\text{OCH}_3$  interacts with the V–OH. During this interaction, the water molecule and the formaldehyde are formed. For these products, an adsorption energy of  $-186.6$  kJ/mol was found. At this stage, a new methanol molecule can be added to the vanadium-zeolite structure (see Figure 4 or the Supporting Information Figure 3). The methanol will interact with the  $\text{VO}-\text{CH}_2$ . During this interaction, the bond between oxygen and  $\text{CH}_2$  is broken and one hydrogen atom is transferred from methanol to the  $\text{CH}_2$ . After the proton transfer, the products dimethyl ether and water result with an adsorption energy of  $-99.2$  kJ/mol. This reaction mechanism was found to occur at a temperature of  $523$  K. At smaller

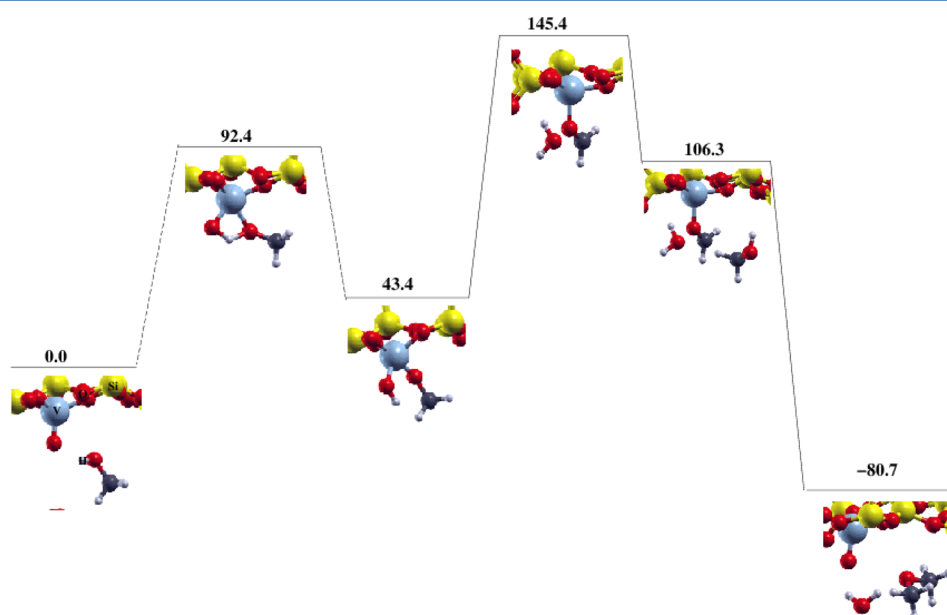


**Figure 4.** Reaction path diagram for Structure 3. The energies for the reactant, intermediate states, and the product are given in kJ/mol.

temperatures (300 K, 415 K) only methoxide product was obtained.

**B. Intrinsic Rate Parameters and Thermodynamic Data.** The adsorption energies calculated for the reactants were found to be between  $-32.9$  ( $-29.7$ ) kJ/mol and  $-49.2$  ( $-44.6$ ) kJ/mol, in close agreement with the results previously reported for the adsorption of methanol on a  $\text{TiO}_2$  supported site ( $-36.4$  and  $-53.6$  kJ/mol).<sup>25</sup> This similarity is due to the fact that the reaction process takes place only near the reactive center ( $\text{VO}_4$  and  $\text{TiO}_2$ , respectively). On the basis of the vibrational frequencies, additionally to the adsorption energies, we have calculated also the adsorption enthalpies at various temperatures  $T = 415/523/650$  K (see Table 2). The

**Table 2. Dispersion Corrected Adsorption Enthalpies for the Reactant Molecules<sup>a</sup>**

molecule	$T$	$\Delta H_{\text{ads,DFT}+D}$
Structure 1	415	-42.1
	523	-41.1
	650	-39.4
Structure 2	415	-39.1
	523	-37.5
	650	-35.5
Structure 3	415	-25.7
	523	-24.1
	650	-22.1

<sup>a</sup>Energies are given in kJ/mol and temperatures in K.

adsorption enthalpies are calculated as the sum of the adsorption energies and the internal energies. As expected, the adsorption enthalpies are decreasing with increasing the temperature. For Structure 2 (Figure 1, Structure 2) adsorption enthalpies between  $-39.2$  and  $-35.4$  kJ/mol are found, while for Structure 3 (Figure 1, Structure 3) the adsorption enthalpies vary between  $-25.7$  and  $-22.1$  kJ/mol for the temperature range 415–650 K. The difference between the adsorption enthalpies of Structure 2 and Structure 3 is 13 kJ/mol. From the adsorption energies a difference of approximately 13 kJ/mol between Structure 2 and Structure 3 is calculated. This shows that Structure 2 is more stable than Structure 3. The orientation of the methanol toward V–OSi group (Structure 2) is more favorable than for the case when the methanol is pointed toward the V=O (Structure 3). The fact that for the adsorption enthalpies a difference of 13 kJ/mol is obtained for Structure 2 and Structure 3 is consistent with the adsorption energy difference obtained for these two structures.

Our results obtained for the energy barriers of methanol oxidation through the three proposed mechanisms,  $\Delta E_{\text{act}} = [69.3$  (56.9)–105.1 (92.4)] kJ/mol, are in good agreement with those previously reported for methanol oxidation on a  $\text{VO}_x/\text{Ti}$  surface, which are in the interval  $\Delta E_{\text{act}} = [69.5$ –119.7] kJ/mol (see Table 3). Similar results were obtained for the methanol oxidized on  $\text{VO}_x/\text{TiO}_2/\text{SiO}_2$  (75.3 kJ/mol),  $\text{VO}_x/\text{ZrO}_2/\text{SiO}_2$  (66.9 kJ/mol),  $\text{VO}_x/\text{CeO}_2/\text{SiO}_2$  (75.3 kJ/mol) and for  $\text{VO}_x/\text{SiO}_2$  (96.2 kJ/mol) (see Table 3). From these results one observes that the various types of surfaces do not considerably change the properties of the oxidation process of methanol ( $\pm 10$ –20 kJ/mol variation is observed for the adsorption and oxidation of methanol on different surfaces). This occurs because the entire reaction takes place only between methanol and the atoms close to vanadium.

**Table 3. DFT Results of Intrinsic Energy Barriers for Methanol Cracking on Different Surfaces<sup>a</sup>**

molecule	$\Delta E_{\text{act,DFT}+D}$
Structure 1/VBEA	75.6 (66.4)
Structure 2/VBEA	69.3 (56.9)
Structure 3/VBEA	105.1 (92.4)
$\text{VO}_x/\text{SiO}_2$	96.2 <sup>(1)</sup>
$\text{VO}_x/\text{TiO}_2/\text{SiO}_2$	75.3 <sup>(1)</sup> –87.9 <sup>(2)</sup>
$\text{VO}_x/\text{ZrO}_2/\text{SiO}_2$	66.9 <sup>(1)</sup>
$\text{VO}_x/\text{CeO}_2/\text{SiO}_2$	75.3 <sup>(1)</sup>
$\text{VO}_x/\text{TiO}_2$	66.9 <sup>(2)</sup>
Structure 1/ $\text{VO}_x/\text{Ti}$	69.5 <sup>(4)</sup>
Structure 2/ $\text{VO}_x/\text{Ti}$	119.7 <sup>(4)</sup>
V-ZSM-5	45 <sup>(3)</sup>

<sup>a</sup>All values are given in kJ/mol. Experimental data from (1) Vining et al.,<sup>32</sup> (2) Vining et al.,<sup>20</sup> (3) Fellah et al.,<sup>19</sup> (4) Gracia et al.<sup>26</sup>. In brackets ZPE (zeropoint vibrational energies) corrected energies are shown.

Comparing the energy barriers obtained for the presently proposed reaction mechanisms (66.4 kJ/mol for the mechanism associated with Structure 1, 56.9 kJ/mol for the mechanism associated with Structure 2, and 92.4 kJ/mol for the mechanism associated with Structure 3) we observe that the mechanisms associated with Structure 1 and Structure 2 have low and close energy barriers compared to Structure 3. The small difference in their energy barriers, correlated with the similarly small difference in the adsorption energies for the reactants, suggests that both these reaction mechanisms are likely to happen. It is to be noted, however, that these reactions do not occur both at the same hydration conditions. Structure 1 is more hydrated and thus more hydrophilic than Structure 2. Structure 3 has a significantly higher energy barrier and therefore its associated reaction mechanism is less probable to happen.

Next to activation energies (Table 3), activation enthalpies ( $\Delta H^\ddagger$ ), entropies ( $\Delta S^\ddagger$ ), Gibbs free energies ( $\Delta G^\ddagger$ ), and reaction rate ( $k^\ddagger$ ) constants have been calculated for all the three mechanisms (Table 4). The calculations have been performed for several temperatures: 415, 523, and 650 K. The 300 K temperature was not considered here as no relevant product could be obtained at this temperature through any mechanism. A difference of about 10 kJ/mol is observed between the intrinsic activation enthalpies of Structure 1 and Structure 2, which is in line with the similar difference for the

**Table 4. Intrinsic Activation Enthalpy, Entropy, Gibbs Free Energy and Rate Constants for Methanol Oxidation on VBEA<sup>a</sup>**

molecule	$T$	$\Delta H_{\text{DFT}}^\ddagger$ (kJ/mol)	$\Delta S_{\text{DFT}}^\ddagger$ (J/mol K)	$\Delta G_{\text{DFT}}^\ddagger$ (kJ/mol)	$k_{\text{DFT}}^\ddagger$ (1/s)
Structure 1	415	62.4	-47.4	82.0	$0.40 \times 10^3$
	523	61.9	-48.4	87.2	$0.21 \times 10^5$
	650	61.4	-49.3	93.4	$0.42 \times 10^6$
Structure 2	415	54.2	-12.6	59.4	$0.28 \times 10^6$
	523	53.4	-14.2	60.9	$0.90 \times 10^7$
	650	52.6	-15.5	62.8	$0.12 \times 10^9$
Structure 3	415	89.3	-16.2	96.1	$0.68 \times 10^1$
	523	88.7	-17.6	97.9	$0.17 \times 10^4$
	650	88.0	-18.8	100.2	$0.11 \times 10^6$

<sup>a</sup>Energies are in kJ/mol, temperatures in K, and  $k$  in  $\text{s}^{-1}$ .

activation energies. Increasing the temperature lowers the activation enthalpies, with a similar amount for both structures.

The intrinsic activation entropies were calculated to be in the range of  $-49.3$  J/mol/K to  $-18.8$  J/mol/K for the three systems, in the temperature interval  $T = 415$ – $650$  K. The calculated activation entropies are always negative and decrease with increasing temperature. The activation entropy is related to the energy-redistribution within the molecule for the reaction to occur. The negative values for the activation entropies, which always occur for bimolecular reactions, indicate that entropy decreases upon achieving the transition state, because the activated complex is more “ordered” than the free molecule. A negative entropy indicates that the activated complex has a lower entropy than the reactants. This is the situation encountered with most bimolecular reactions because two molecules, initially in a random situation, must come together with resulting loss of entropy. A positive value of entropy is usually associated with dissociation or fragmentation reactions or with those processes in which there is a greater disorganization in the transition state than in the reactants.

**C. Experimental Results. C.1. Acidity of  $V_x$ SiBEA Zeolites: FT-IR Investigation.** The treatment of TEABEA zeolite by aqueous  $\text{HNO}_3$  solution to remove framework Al atoms leads to the appearance in the FT-IR spectrum of SiBEA (Figure 5)

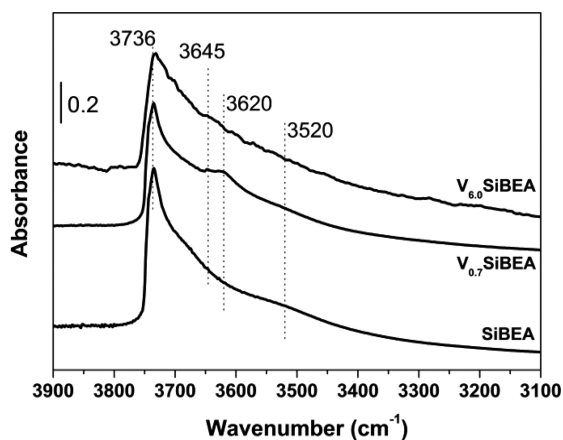


**Figure 5.** FT-IR spectra recorded at room temperature of SiBEA,  $V_{0.7}$ SiBEA and  $V_{6.0}$ SiBEA.

with an intense band at  $3736\text{ cm}^{-1}$  and a broad band at  $3520\text{ cm}^{-1}$  due to isolated internal and H-bonded silanols, respectively, present in vacant T atom sites, in agreement with earlier assignments.<sup>23,91,92</sup>

After contact of SiBEA with aqueous  $\text{NH}_4\text{VO}_3$  solution at  $\text{pH} = 2.5$ , two bands appear at  $3645$  and  $3620\text{ cm}^{-1}$  for  $V_{0.7}$ SiBEA assigned to the hydroxyl vibration of framework  $(\text{SiO})_2(\text{HO})\text{V}=\text{O}$  species located at two different crystallographic sites, in line with earlier data for VSiBEA zeolite.<sup>93,94</sup> As shown in Figure 5, the intensity of these bands significantly decreases from  $V_{0.7}$ SiBEA to  $V_{6.0}$ SiBEA suggesting that for latter sample a major part of vanadium is present as extra-framework polynuclear V species. Their presence in  $V_{6.0}$ SiBEA sample reduces strongly the intensity of the band at  $3645$  and  $3620\text{ cm}^{-1}$  corresponding to isolated  $(\text{SiO})_2(\text{HO})\text{V}=\text{O}$  species.

To determine the acidity of SiBEA,  $V_{0.7}$ SiBEA, and  $V_{6.0}$ SiBEA, the FT-IR spectra of adsorbed pyridine used as probe molecule were recorded. Table 5 shows a very small

**Table 5. Number of Acidic Centers in SiBEA,  $V_{0.7}$ SiBEA, and  $V_{6.0}$ SiBEA Zeolites (Related to 10 mg of Catalyst) Determined from the Amount of Pyridine Remaining Adsorbed after Outgassing the Samples at 473 K (Number of Lewis or Brønsted Acidic Centers) and at 473 and 523 K (Total Number of Acidic Centers)**

sample	Lewis acidic centers ( $\times 10^{17}$ )	Brønsted acidic centers ( $\times 10^{17}$ )	total no. acidic centers ( $\times 10^{17}$ )	
			473 K	523 K
SiBEA	5.7	8.7	14.4	
$V_{0.7}$ SiBEA	315.7	57.8	373.5	216.7
$V_{6.0}$ SiBEA	268.0	141.2	409.2	254.1

amount of Lewis and Brønsted acidic sites for SiBEA, most probably related to  $\text{Al}^{3+}$  ions and the acidic proton of  $\text{Al}-\text{O}(\text{H})-\text{Si}$  groups, respectively, still present after treatment of BEA zeolite with nitric acid. In contrast, for  $V_{0.7}$ SiBEA zeolites additional Lewis and Brønsted acidic sites are generated. As reported earlier for BEA zeolite,<sup>23</sup> the additional Brønsted acidic centers observed after modification with vanadium (e.g., in  $V_{0.7}$ SiBEA) are related to the acidic proton of the OH group of framework hydroxylated  $(\text{SiO})_2(\text{HO})\text{V}=\text{O}$ .<sup>8</sup> This can be deduced from disappearance of IR band assigned to  $(\text{SiO})_2(\text{HO})\text{V}=\text{O}$  after pyridine adsorption. However, as described earlier for BEA and sodalite systems, only a small part of all framework tetrahedral V(V) species appear as  $(\text{SiO})_2(\text{HO})\text{V}=\text{O}$ .<sup>95</sup>

The number of acidic centers in  $V_x$ SiBEA calculated from the amount of pyridine left on the zeolite surface after outgassing at 473 K for 0.5 h is given in Table 5. The number of Brønsted acidic centers increases with the vanadium content but not in the directly proportional way. On the other hand, the number of Lewis acidic centers significantly decreases from  $V_{0.7}$ SiBEA to  $V_{6.0}$ SiBEA suggesting that for latter sample a major part of vanadium is present as extra-framework polynuclear V. This of course reduces the amount of isolated mononuclear V to a high extent. The total number of acidic centers determined from the amount of pyridine remaining adsorbed after outgassing of the samples at 523 K is also presented in Table 5. These data make the estimation of acid strength possible. There is a large difference in the acid strength between the parent SiBEA and the resulting V-containing zeolites. Thus, the strength of acidic centers related to vanadium species in both  $V_{0.7}$ SiBEA and  $V_{6.0}$ SiBEA appears to be higher than the strength of acidic centers present in SiBEA zeolite.

**C.2. Nature and Environment of Vanadium in  $V_x$ SiBEA: DR UV-Visible.** The DR UV-visible spectra of  $V_x$ SiBEA are shown in Figure 6. The absence of the d-d band expected for  $V^{IV}$  ( $3d^1$ ) ions for  $V_{0.7}$ SiBEA and  $V_{6.0}$ SiBEA in the range 600–800 nm suggests that there are no  $V^{IV}$  ions. For  $V_{0.7}$ SiBEA, two broad bands are observed at 265 and 340 nm which can be attributed to oxygen-pseudotetrahedral V(V) charge transfer (CT) transitions, involving bridging (V–O–Si) and terminal (V=O) oxygens, respectively, in line with earlier results.

For  $V_{6.0}$ SiBEA with much higher V content, the bands at 280, 320, 410, and 465 nm are observed involving framework mononuclear pseudotetrahedral V(V) (the bands at 280 and 320 nm) and extra-framework polynuclear V(V) (the bands at 410 and 465 nm).

**C.3. Catalytic Activity of  $V_x$ SiBEA in Oxidation of Methanol.** As reported earlier,<sup>96</sup> acidic and basic centers play

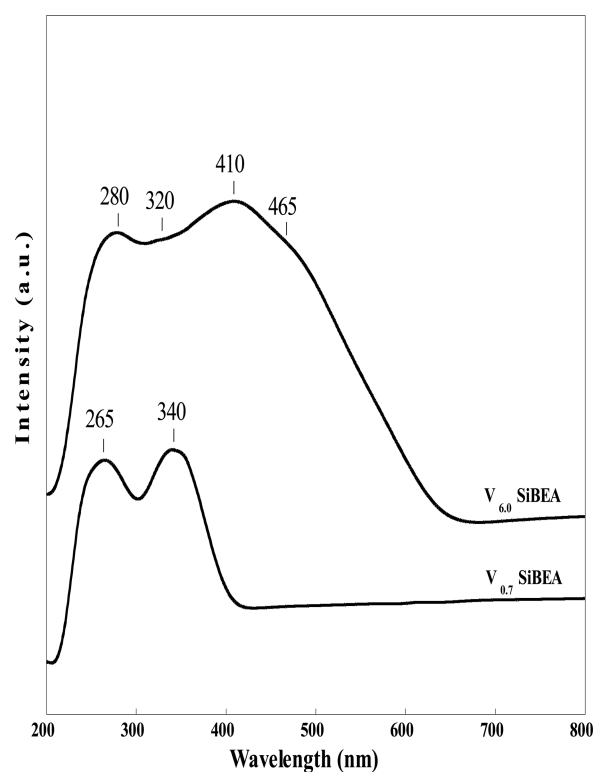


**Figure 6.** DR UV-vis spectra recorded at room temperature of  $V_{0.7}$ SiBEA and  $V_{6.0}$ SiBEA.

a role in the oxidation of methanol by oxide catalysts. In  $V_x$ SiBEA zeolites, framework non-hydroxylated  $(\text{SiO})_3\text{V}=\text{O}$  and hydroxylated  $(\text{SiO})_2(\text{HO})\text{V}=\text{O}$  behave as either redox or Lewis ( $\text{V}^{5+}$ ) and Brønsted acidic (proton of the OH group) and basic ( $\text{O}^{2-}$ ) centers on which hydrogen abstraction can take place, as proposed earlier.<sup>23</sup>

The first step in methanol oxidation is suggested to be the abstraction of hydrogen from methanol leading to methoxy groups<sup>96</sup> that further transform depending on the kind and strength of active centers, as reported earlier.<sup>97</sup> In the presence of acidic centers only, methoxy groups interact with a second  $\text{CH}_3\text{OH}$  molecule to form dimethyl ether.

The results of methanol oxidation are given in Table 6 which gather the conversion and selectivity of SiBEA,  $V_{0.7}$ SiBEA and  $V_{6.0}$ SiBEA zeolites. The SiBEA exhibits a very small number of acidic centers (Table 5) and leads to dimethyl ether only, with methanol conversion of 5% (Table 6). The absence of vanadium species and basic centers in SiBEA seems to explain the absence of oxidation products.

The incorporation of a small amount of vanadium in  $V_{0.7}$ SiBEA does not change the methanol conversion, it however shifts the selectivity toward partial oxidation products

(Table 6), typical of the redox and acid–base character of  $V_x$ SiBEA. The selectivity to dimethyl ether decreases from 100% for SiBEA to 62% for  $V_{0.7}$ SiBEA. Total oxidation to  $\text{CO}_2$ , which requires the presence of highly basic centers, is not significant on both  $V_x$ SiBEA samples.

The increase of V content in  $V_{6.0}$ SiBEA zeolite leads to an increase of methanol conversion and selectivity toward formaldehyde (Table 6). As suggested earlier,<sup>23</sup> formaldehyde chemisorbed on acidic centers can desorb as such or be further transformed to formate species.

The presence of basic vanadyl oxygen in the neighborhood of vanadium is required to transform methoxy species into formaldehyde by hydrogen abstraction. This vanadyl oxygen is also involved in the redox cycle of vanadium in the further transformation of chemisorbed formaldehyde into partial oxidation products (e.g., methyl formate). However, the reaction pathway depends on the strength of acidic centers, thus the lower their strength, the easier is the desorption of formaldehyde. The incorporation of vanadium into SiBEA generates both new Lewis acidic and basic oxygen centers ( $\text{V}^{5+}=\text{O}^{2-}$ ) as shown by the increase of the number of Lewis acidic centers (Table 5). On the other hand, the increase of BAS number suggests the formation of framework hydroxylated  $(\text{SiO})_2(\text{HO})\text{V}=\text{O}$ .

As proposed earlier,<sup>23</sup> the basic vanadyl oxygen of framework  $(\text{SiO})_3\text{V}=\text{O}$  and  $(\text{SiO})_2(\text{HO})\text{V}=\text{O}$  is able to abstract hydrogen from methoxy groups to form formaldehyde, but because of the high nucleophilicity of the basic vanadyl oxygen,  $(\text{SiO})_3\text{V}=\text{O}$  can strongly chemisorb formaldehyde and lead to its full oxidation. However, a very little amount of  $\text{CO}_2$  formed in methanol oxidation (2 and 1% on  $V_{0.7}$ SiBEA and  $V_{6.0}$ SiBEA, respectively) suggests that framework  $(\text{SiO})_3\text{V}=\text{O}$  are rather not involved in methanol oxidation (Table 6). In contrast, on the less nucleophilic basic vanadyl oxygen of the framework  $(\text{SiO})_2(\text{HO})\text{V}=\text{O}$ , formaldehyde being less strongly chemisorbed can desorb. The proton of framework  $(\text{SiO})_2(\text{OH})\text{V}=\text{O}$  is likely to be totally responsible for the Brønsted acidity of  $V_x$ SiBEA zeolites, where a small part of BAS comes from residual  $\text{Al}-\text{O}(\text{H})-\text{Si}$ . The methoxy species formed on Lewis or Brønsted acidic centers can further react with a  $\text{CH}_3\text{OH}$  molecule to form dimethyl ether or can be transformed into formaldehyde in the presence of basic centers, which abstract hydrogen. For these two reasons, dimethyl ether and formaldehyde are the main products in methanol oxidation on  $V_x$ SiBEA.

The formaldehyde yield increases significantly with vanadium loading, from 0.75 to 11.7% for  $V_{0.7}$ SiBEA and  $V_{6.0}$ SiBEA, respectively. This suggests that framework  $(\text{SiO})_2(\text{HO})\text{V}=\text{O}$  are mainly involved in the transformation of methanol via oxidation path. In contrast, the dimethyl ether yield increases less than twice, suggesting that dimethyl ether formation does not occur mainly on V sites. In our opinion, the dimethyl ether

**Table 6.** Conversion and Selectivity Determined at 523 K for Methanol Oxidation on  $V_x$ SiBEA<sup>a</sup>

catalyst	methanol conversion, %	selectivity, %				
		$(\text{CH}_3)_2\text{O}$	HCHO	$(\text{CH}_3\text{O})_2\text{CH}_2$	$\text{HCOOCH}_3$	$\text{CO}_2$
SiBEA	5	100				
$V_{0.7}$ SiBEA	5	62	15	2	19	2
$V_{6.0}$ SiBEA	21	26	56	2	15	1

<sup>a</sup>Mass of catalyst, 40 mg; activation temperature in argon, 673 K; total reactant flow, 40 mL/min (Ar, 35.2 mL/min;  $\text{O}_2$ , 3.2 mL/min; MeOH, 1.6 mL/min;  $\text{O}_2/\text{MeOH}$  molar ratio = 2).

formation takes place on Brønsted acidic sites and is most likely related to the acidic proton of Al–O(H)–Si groups, present as traces in SiBEA (Table 5).

The comparison of the experimental results with those from ref.<sup>23</sup> shows that the catalytic activity of VSiBEA zeolites in methanol oxidation is strongly related to the presence of hydroxylated  $(\text{SiO})_2(\text{HO})\text{V}=\text{O}$  species.

The differences in methanol conversion and selectivity to  $(\text{CH}_3)_2\text{O}$  and HCHO on  $\text{V}_{0.7}\text{SiBEA}$  zeolite catalyst could be related to different states of SiBEA obtained after treatment with concentrated nitric acid solution. The higher conversion of methanol and lower selectivity to formaldehyde observed in the present study suggests that in SiBEA there are more traces of (Al–O(H)–Si) strong Brønsted acid sites. These sites are responsible for the conversion of methanol to methyl ether which was not completely removed upon treatment with  $\text{HNO}_3$ .

In contrast, the lower conversion of methanol and higher selectivity to formaldehyde in ref 23 suggests that in SiBEA there were less traces of strong Brønsted acid sites. Indeed, the Si/Al ratio of 1000 indicates that in both SiBEA supports (present and previous) obtained upon treatment with  $\text{HNO}_3$  there are only about 200–300 ppm of Al present, an amount that is very difficult to measure precisely by chemical analysis.

**Difference between Hydroxylated and Non-hydroxylated V Species Present in VSiBEA.** In this section the difference between the methanol oxidation on the three constructed structures are discussed. The reaction mechanism corresponding to the methanol oxidation involves two main steps: (1) oxidation, requiring oxygen either from the gas phase or from the catalyst and (2) dehydration.

For the SiBEA catalyst only the production of dimethyl ether has been observed experimentally. Introducing a vanadium atom into the system leads to a reduction of the concentration of dimethyl ether and an increase of different products such as formaldehyde. Vanadium based species exhibit significant activity in methanol oxidation. For a higher concentration of vanadium,  $\text{V}_{6.0}\text{SiBEA}$ , the dimethyl ether has been found to be 26% and formaldehyde 56%.

Two types of reactions were considered: (1) occurring on the hydroxylated V species of VSiBEA and (2) occurring on the non-hydroxylated V species of VSiBEA.

The hydroxylated V species present in VSiBEA corresponds to Structure 1. For constructing the hydroxylated  $(\text{SiO})_2(\text{HO})\text{V}=\text{O}$  in VSiBEA, one V–OSi has been replaced by V–OH. Now, the vanadium is connected with two OSi groups, one OH, and a double oxygen bond.

The non-hydroxylated  $(\text{SiO})_3\text{V}=\text{O}$  in VSiBEA corresponds to Structure 2 and Structure 3. The vanadium is connected with three OSi groups and the double bond oxygen.

In correspondence with the experimental data for all the systems, both the formaldehyde and the dimethyl ether have been found. The temperature at which the products were obtained in our simulations is in good agreement with the temperature in the experiments. The first step in the reaction mechanism is the detachment of one hydrogen atom from the methanol and the formation of the methoxy group. For this step, a small energy barrier was shown to be present: 66.4 kJ/mol for the hydroxylated  $(\text{SiO})_2(\text{HO})\text{V}=\text{O}$  in VSiBEA and 56.9 kJ/mol for the non-hydroxylated  $(\text{SiO})_3\text{V}=\text{O}$  in VSiBEA. The small energy barriers can be explained as the transfer of one hydrogen from methanol to V on VSiBEA, since this transfer should not require too much energy. Because of the

similar values for the energy barriers it is hard to determine whether the hydroxylated or the non-hydroxylated V species are more appropriate for the reaction mechanism.

The environment of active sites strongly affects activity and selectivity. The high selectivity toward formaldehyde is observed when the nucleophilicity of oxygen present in the neighborhood of vanadium is moderate.<sup>23</sup> For the non-hydroxylated  $(\text{SiO})_3\text{V}=\text{O}$  of VSiBEA, formaldehyde formation has been calculated. However, the high nucleophilicity of the vanadyl oxygen can lead in this case to strong chemisorption of formaldehyde followed by the formation of other products, e.g. methylal, which can be transformed into methyl formate by further reaction with methanol. A further increase in nucleophilicity causes the total oxidation of methanol.<sup>23</sup>

For the hydroxylated  $(\text{SiO})_2(\text{HO})\text{V}=\text{O}$  present in VSiBEA, a very small amount (approximately 2%) of  $\text{CO}_2$  has been observed experimentally. In Figure 2, the methoxy group can interact with methanol and form dimethyl ether and water. From the simulations, the adsorption energy for these products is  $-111.6$  kJ/mol, being smaller than the values reported for the non-hydroxylated structure. The dimethyl ether can be further transformed into formaldehyde in the presence of the basic centers, which abstract hydrogen.

## CONCLUSIONS

Theoretical and experimental investigations for the oxidation of methanol on VSiBEA zeolite have been performed in the present work. Three different systems have been investigated using DFT, including dispersion interactions. The different calculated thermodynamic properties are in good agreement with the experimental and other published theoretical data.

The products obtained are formaldehyde, dimethyl ether, and water. By the use of TPS and molecular dynamics, we were able to follow the reaction pathway of the systems at three different temperatures ( $T = 300, 415, \text{ and } 523$  K). All intermediates and products are reported. At a temperature of 523 K, the formation of the products is possible for all the three considered structures, albeit with different energy barriers. For Structure 2 the formation of formaldehyde is possible at 415 K due to the low activation energy.

The experimental investigations allowed the determination of the acidic properties of VSiBEA zeolites (FT-IR with pyridine as molecule probe) and the nature and environment of V species. The experimental investigations of the methanol oxidation are in line with the theoretical investigation presented in this work.

## ASSOCIATED CONTENT

### Supporting Information

Structural values for Structure 1, Structure 2, and Structure 3 and structures for reactant, transition states, intermediate states, and products. The Supporting Information is available free of charge on the ACS Publications website at DOI: 10.1021/acs.jpcc.5b01911.

## AUTHOR INFORMATION

### Corresponding Authors

\*E-mail: diana.tranca@tu-harburg.de.

\*E-mail: keil@tu-harburg.de.

\*E-mail: stanislaw.dzwigaj@upmc.fr.

### Notes

The authors declare no competing financial interest.

<sup>†</sup>M.C. is a member of the Institut Universitaire de France.

## ACKNOWLEDGMENTS

D.C.T. acknowledges support from HPC-Europa2++ (Grant 799) for mobility as well as for high-performance computing time at GENCI- [CCRT/CINES/IDRIS] (Grant 2013-[x2013082022]). This work was also performed by using the HPC resources on the Juropa supercomputer at the Forschungszentrum Jülich (Germany), CCRE at Université Pierre et Marie Curie (France), and on HLRN in Hannover (Germany).

## REFERENCES

- (1) Tielens, F.; Calatayud, M.; Dzwigaj, S.; Che, M. What do Vanadium Framework Sites Look Like in Redox Model Silicate Zeolites? *Microporous Mesoporous Mater.* **2009**, *119*, 137–143.
- (2) Gonzalez-Navarrete, P.; Gracia, L.; Calatayud, M.; Andres, J. Density Functional Theory Study of the Oxidation of Methanol to Formaldehyde on a Hydrated Vanadia Cluster. *J. Comput. Chem.* **2010**, *31*, 2493–2501.
- (3) Corma, A. State of the Art and Future Challenges of Zeolites as Catalysts. *J. Catal.* **2003**, *216*, 298–312.
- (4) Horsley, J. A. Producing Bulk and Fine Chemicals Using Solid Acids. *CHEMTECH* **1997**, *27*, 45–49.
- (5) Stoeker, M. Gas Phase Catalysis by Zeolites. *Microsc. Mesop. Materials* **2005**, *82*, 257–292.
- (6) Matsuda, T.; Kikuchi, E. Synthesis of Symmetrical Alkyl-Aromatics by use of Shape Selective Catalysts. *Res. Chem. Intermed.* **1993**, *19*, 319–332.
- (7) Heinz, F. Selective Hydrocarbon Oxidation in Zeolites. *Science* **2006**, *313*, 309–310.
- (8) Larsen, S. C. Applications of Zeolites in Environmental Catalysis. In *Environmental Catalysis*; Grassian, V. H., Ed.; CRC Press: Boca Raton, FL, 2005.
- (9) Mignon, P.; Pidko, E. A.; Van Santen, R. A.; Geerlings, P.; Schoonheydt, R. A. Understanding the Reactivity and Basicity of Zeolites: A Periodic DFT Study of the Disproportionation of N<sub>2</sub>O<sub>4</sub> on Alkali-Cation-Exchanged Zeolite Y. *Chem.—Eur. J.* **2008**, *14*, 5168–5177.
- (10) Corma, A. Inorganic Solid Acids and Their Use in Acid-Catalyzed Hydrocarbon Reactions. *Chem. Rev.* **1995**, *95*, 559–614.
- (11) Vermeiren, W.; Gilson, J.-P. Impact of Zeolites on the Petroleum and Petrochemical Industry. *Top. Catal.* **2009**, *52*, 1131–1161.
- (12) Zimmerman, P. M.; Tranca, D. C.; Gomes, J.; Lambrecht, D. S.; Head-Gordon, M.; Bell, A. T. Ab Initio Simulations Reveal that Reaction Dynamics Strongly Affect Product Selectivity for the Cracking of Alkanes over H-MFI. *J. Am. Chem. Soc.* **2012**, *134*, 19468–19476.
- (13) Tranca, D. C.; Hansen, N.; Swisher, J. A.; Smit, B.; Keil, F. J. Combined Density Functional Theory and Monte Carlo Analysis of Monomolecular Cracking of Light Alkanes Over H-ZSM-5. *J. Phys. Chem. C* **2012**, *116*, 23408–23417.
- (14) Tielens, F.; Calatayud, M. The Synergistic Power of Theory and Experiment in the Field of Catalysis Preface. *Catal. Today* **2011**, *177*, 1–2.
- (15) Tielens, F. Exploring the Reactivity of Intraframework Vanadium, Niobium and Tantalum Sites in Zeolitic Materials Using the Molecular Electrostatic Potential. *J. Mol. Struct.—Theochem* **2009**, *903*, 23–27.
- (16) Tielens, F. Exploring the Reactivity of Framework Vanadium, Niobium, and Tantalum Sites in Zeolitic Materials Using DFT Reactivity Descriptors. *J. Comput. Chem.* **2009**, *30*, 1946–1951.
- (17) Wojtaszek, A.; Ziolek, M.; Dzwigaj, S.; Tielens, F. Comparison of Competition between T = O and T-OH Groups in Vanadium, Niobium, Tantalum BEA zeolite and SOD based Zeolites. *Chem. Phys. Lett.* **2011**, *514*, 70–73.

(18) Wojtaszek, A.; Ziolek, M.; Tielens, F. Probing Acid-Base Properties in Group V Aluminum Containing Zeolites. *J. Phys. Chem. C* **2012**, *116*, 2462–2468.

(19) Fella, M. F.; Onal, I. A DFT study on the [VO]<sup>1+</sup> - ZSM-5 Cluster: Direct Methanol Oxidation to Formaldehyde by N<sub>2</sub>O. *Phys. Chem. Chem. Phys.* **2013**, *15*, 13969–13977.

(20) Vining, W. C.; Goodrow, A.; Strunk, J.; Bell, A. T. An Experimental and Theoretical Investigation of the Structure and Reactivity of Bilayered VO<sub>x</sub>/TiO<sub>x</sub>/SiO<sub>2</sub> Catalysts for Methanol Oxidation. *J. Catal.* **2010**, *270*, 163–171.

(21) Goodrow, A.; Bell, A. T. A Theoretical Investigation of the Selective Oxidation of Methanol to Formaldehyde on Isolated Vanadate Species Supported on Silica. *J. Phys. Chem. C* **2007**, *111*, 14753–14761.

(22) Khaliullin, R. Z.; Bell, A. T. A Density Functional Theory Study of the oxidation of Methanol to Formaldehyde over Vanadia Supported on Silica, Titania and Zirconia. *J. Phys. Chem. B* **2002**, *106*, 7832–7838.

(23) Trejda, M.; Ziolek, M.; Millot, Y.; Chalupka, K.; Che, M.; Dzwigaj, S. Methanol Oxidation on VSiBEA Zeolites: Influence of V Content on the Catalytic Properties. *J. Catal.* **2011**, *281*, 169–176.

(24) Martin, A.; Luecke, B. Ammoxidation and Oxidation of Substituted Methyl Aromatics on Vanadium-Containing Catalysts. *Catal. Today* **2000**, *57*, 61–70.

(25) Gonzalez-Navarrete, P.; Gracia, L.; Calatayud, M.; Andres, J. Unraveling the Mechanisms of the Selective Oxidation of Methanol to Formaldehyde in Vanadia Supported on Titania Catalyst. *J. Phys. Chem. C* **2010**, *114*, 6039–6046.

(26) Gracia, L.; Gonzalez-Navarrete, P.; Calatayud, M.; Andres, J. A DFT Study of Methanol Dissociation on Isolated Vanadate Groups. *Catal. Today* **2008**, *139*, 214–220.

(27) Robert, H.; George, G.; Seaman, C. *Kirk-Othmer Encyclopedia of Chemical Technology*, 3rd ed.; Wiley: Hoboken, NJ, 2005; Vol. 12.

(28) Louwerse, M. J.; Vassilev, P.; Baerends, E. J. Oxidation of Methanol by FeO<sup>2+</sup> in Water: DFT Calculations in the Gas Phase and Ab Initio MD Simulations in Water Solution. *J. Phys. Chem. A* **2008**, *112*, 1000–1012.

(29) Yoshizawa, K.; Shiota, Y.; Kagawa, Y.; Yamabe, T. Femtosecond Dynamics of the Methane–Methanol and Benzene–Phenol Conversions by an Iron–Oxo Species. *J. Phys. Chem. A* **2000**, *104*, 2552–2561.

(30) Romanyshyn, Y.; Guimond, S.; Kuhlbeck, H.; Kaya, S.; Blum, R. P.; Niehus, H.; Shaikhutdinov, S.; Simic-Milosevic, V.; Nilius, N.; Freund, H. J.; Ganduglia-Pirovano, M. V.; et al. Selectivity in Methanol Oxidation as Studied on Model Systems Involving Vanadium Oxides. *Top. Catal.* **2008**, *50*, 106–115.

(31) Dobler, J.; Pritzsche, M.; Sauer, J. Oxidation of Methanol to Formaldehyde on Supported Vanadium Oxide Catalysts Compared to Gas Phase Molecules. *J. Am. Chem. Soc.* **2005**, *127*, 10861–10868.

(32) Vining, W. C.; Strunk, J.; Bell, A. T. Investigation of the Structure and Activity of VO<sub>x</sub>/CeO<sub>2</sub>/SiO<sub>2</sub> Catalysts for Methanol Oxidation to Formaldehyde. *J. Catal.* **2012**, *285*, 160–167.

(33) Witko, M.; Tokarz, R.; Haber, R. Vanadium Pentoxide. II. Quantum Chemical Modeling. *Appl. Catal., A* **1997**, *157*, 23–44.

(34) Hermann, K.; Witko, M.; Druzinic, R.; Tokarz, R. Oxygen Vacancies at Oxide Surfaces: Ab Initio Density Functional Theory Studies on Vanadium Pentoxide. *Appl. Phys. A: Mater. Sci. Process* **2001**, *72*, 429–442.

(35) Kachurovskaya, N. A.; Mikheeva, E. P.; Zhidomirov, G. M. Cluster Molecular Modeling of Strong Interaction for VO<sub>x</sub>/TiO<sub>2</sub> Supported Catalyst. *J. Mol. Catal. A* **2002**, *178*, 191–198.

(36) Calatayud, M.; Mguig, B.; Minot, C. A Periodic Model for the V<sub>2</sub>O<sub>5</sub>–TiO<sub>2</sub> (Anatase) Catalyst. Stability of Dimeric Species. *Surf. Sci.* **2003**, *526*, 297–308.

(37) Vittadini, A.; Selloni, A. Periodic Density Functional Theory Studies of Vanadia–Titania Catalysts: Structure and Stability of the Oxidized Monolayer. *J. Phys. Chem. B* **2004**, *108*, 7337–7343.

(38) Brazdova, V.; Ganduglia-Pirovano, M. V.; Sauer, J. Periodic Density Functional Study on Structural and Vibrational Properties of

Vanadium Oxide Aggregates. *Phys. Rev. B* **2004**, *69*, 165420 (14 pages).

(39) Ganduglia-Pirovano, M. V.; Sauer, J. Stability of Reduced  $V_2O_5(001)$  Surfaces. *Phys. Rev. B* **2004**, *70*, 045422 (13 pages).

(40) Islam, M. M.; Costa, D.; Calatayud, M.; Tielens, F. Characterization of Supported Vanadium Oxide Species on Silica: A Periodic DFT Investigation. *J. Phys. Chem. C* **2009**, *113*, 10740–10746.

(41) Calatayud, M.; Mguig, B.; Minot, C. Modeling Catalytic Reduction of NO by Ammonia over  $V_2O_5$ . *Surf. Sci. Rep.* **2004**, *55*, 169–236.

(42) Kresse, G.; Hafner, J. *Ab initio* Molecular Dynamics for Liquid Metals. *Phys. Rev. B* **1993**, *47*, 558–561.

(43) Kresse, G.; Furthmüller, J. Efficiency of *Ab-Initio* Total Energy Calculations for Metals and Semiconductors Using a Plane-Wave Basis Set. *Computat. Mater. Sci.* **1996**, *6*, 15–50.

(44) Kresse, G.; Furthmüller, J. Efficient Iterative Schemes for *Ab Initio* Total-Energy Calculations Using a Plane-Wave Basis Set. *Phys. Rev. B* **1996**, *54*, 11169–11186.

(45) Kresse, G.; Joubert, D. From Ultrasoft Pseudopotentials to the Projector Augmented-Wave Method. *Phys. Rev. B* **1999**, *59*, 1758–1775.

(46) Blöchl, P. E. Projector Augmented-Wave Method. *Phys. Rev. B* **1994**, *50*, 17953–17979.

(47) Newsam, J. M.; Treacy, M. M. J.; Koetsier, W. T.; de Gruyeter, C. B. Structural Characterization of Zeolite Beta. *Proc. R. Soc. London A* **1988**, *420*, 375–405.

(48) Wojtaszek, A.; Ziolk, M.; Dzwigaj, S.; Tielens, F. Comparison of Competition between T = O and T–OH Groups in Vanadium, Niobium, Tantalum BEA Zeolite and SOD Based Zeolites. *Chem. Phys. Lett.* **2011**, *514*, 70–73.

(49) Heyden, A.; Bell, A. T.; Keil, F. J. Efficient Methods for Finding Transition States in Chemical Reactions: Comparison of Improved Dimer Method and Partitioned Rational Function Optimization Method. *J. Chem. Phys.* **2005**, *123*, 224101 (14 pages).

(50) Bucko, T.; Benco, L.; Dubay, O.; Dellago, C.; Hafner, J. Mechanism of Alkane Dehydrogenation Catalyzed by Acidic Zeolites: *Ab initio* Transition Path Sampling. *J. Chem. Phys.* **2009**, *131*, 214508 (11 pages).

(51) Bucko, T.; Hafner, J. Entropy Effects in Hydrocarbon Conversion Reactions: Free-Energy Integrations and Transition-Path Sampling. *J. Phys.: Condens. Matter.* **2010**, *22*, 384201 (10 pages).

(52) Wesolowski, T. A.; Parisel, O.; Ellinger, Y.; Weber, J. Comparative Study of Benzene...X (X = O<sub>2</sub>, N<sub>2</sub>, CO) Complexes Using Density Functional Theory: The Importance of an Accurate Exchange–Correlation Energy Density at High Reduced Density Gradients. *J. Phys. Chem. A* **1997**, *101*, 7818–7825.

(53) Zhang, Y.; Pan, W.; Yang, W. Describing van der Waals Interaction in Diatomic Molecules with Generalized Gradient Approximations: The Role of the Exchange Functional. *J. Chem. Phys.* **1997**, *107*, 7921–7925.

(54) Gritsenko, O. V.; Ensing, B.; Schipper, P. R. T.; Baerends, E. J. Comparison of the Accurate Kohn–Sham Solution with the Generalized Gradient Approximations (GGAs) for the S<sub>N</sub>2 Reaction F<sup>−</sup> + CH<sub>3</sub>F → FCH<sub>3</sub> + F<sup>−</sup>: A Qualitative Rule To Predict Success or Failure of GGAs. *J. Phys. Chem. A* **2000**, *104*, 8558–8565.

(55) Porezag, D.; Pederson, M. R. Density Functional Based Studies of Transition States and Barriers for Hydrogen Exchange and Abstraction Reactions. *J. Chem. Phys.* **1995**, *102*, 9345–9349.

(56) Perdew, J. P.; Zunger, A. Self-Interaction Correction to Density-Functional Approximations for Many-Electron Systems. *Phys. Rev. B* **1981**, *23*, 5048–5079.

(57) Kümmel, S.; Kronik, L. Orbital-Dependent Density Functionals: Theory and Applications. *Rev. Mod. Phys.* **2008**, *80*, 3–60.

(58) Furche, F. Molecular Tests of the Random Phase Approximation to the Exchange–Correlation Energy Functional. *Phys. Rev. B* **2001**, *64*, 195120 (8 pages).

(59) Harl, J.; Kresse, G. Cohesive Energy Curves for Noble Gas Solids Calculated by Adiabatic Connection Fluctuation-Dissipation Theory. *Phys. Rev. B* **2008**, *77*, 045136 (8 pages).

(60) Dion, M.; Rydberg, H.; Schroeder, E.; Langreth, D. C.; Lundqvist, B. I. Van der Waals Density Functional for General Geometries. *Phys. Rev. Lett.* **2004**, *92*, 246401 (4 pp).

(61) Grimme, S. Accurate Description of van der Waals Complexes by Density Functional Theory Including Empirical Corrections. *J. Comput. Chem.* **2004**, *25*, 1463–1473.

(62) Grimme, S. Semiempirical GGA-Type Density Functional Constructed with a Long-Range Dispersion Correction. *J. Comput. Chem.* **2006**, *27*, 1787–1799.

(63) Grimme, S.; Antony, J.; Ehrlich, S.; Krieg, H. A Consistent and Accurate *Ab Initio* Parametrization of Density Functional Dispersion Correction (DFT-D) for the 94 Elements H–Pu. *J. Chem. Phys.* **2010**, *132*, 154104 (19 pages).

(64) Grimme, S.; Ehrlich, S.; Goerigk, L. Effect of Damping Function in Dispersion Corrected Density Functional Theory. *J. Comput. Chem.* **2011**, *32*, 1456–1465.

(65) Tkatchenko, A.; Scheffler, M. Accurate Molecular Van Der Waals Interactions from Ground-State Electron Density and Free-Atom Reference Data. *Phys. Rev. Lett.* **2009**, *102*, 073005 (4 pages).

(66) Jurecka, P.; Cerny, J.; Hobza, P.; Salahub, D. R. Density Functional Theory Augmented with an Empirical Dispersion Term. Interaction Energies and Geometries of 80 Noncovalent Complexes Compared with *Ab Initio* Quantum Mechanics Calculations. *J. Comput. Chem.* **2007**, *28*, 555–569.

(67) Ortmann, F.; Bechstedt, F.; Schmidt, W. G. Semiempirical van der Waals Correction to the Density Functional Description of Solids and Molecular Structures. *Phys. Rev. B* **2006**, *73*, 205101 (10 pages).

(68) Zimmerli, U.; Parrinello, M.; Koumoutsakos, P. Dispersion Corrections to Density Functionals for Water Aromatic Interactions. *J. Chem. Phys.* **2004**, *120*, 2693–2699.

(69) Wu, Q.; Yang, W. Empirical Correction to Density Functional Theory for van der Waals Interactions. *J. Chem. Phys.* **2002**, *116*, 515–524.

(70) Svelle, S.; Tuma, C.; Rozanska, X.; Kerber, T.; Sauer, J. Quantum Chemical Modeling of Zeolite-Catalyzed Methylation Reactions: Toward Chemical Accuracy for Barriers. *J. Am. Chem. Soc.* **2009**, *131*, 816–825.

(71) Cheng, L.; Curtiss, L. A.; Assary, R. S.; Greeley, J.; Kerber, T.; Sauer, J. Adsorption and Diffusion of Fructose in Zeolite HZSM-5: Selection of Models and Methods for Computational Studies. *J. Phys. Chem. C* **2011**, *115*, 21785–21790.

(72) Kerber, T.; Sierka, M.; Sauer, J. Application of Semiempirical Long-Range Dispersion Corrections to Periodic Systems in Density Functional Theory. *J. Comput. Chem.* **2008**, *29*, 2088–2097.

(73) Hansen, N.; Kerber, T.; Sauer, J.; Bell, A. T.; Keil, F. J. Quantum Chemical Modeling of Benzene Ethylation over H-ZSM-5 Approaching Chemical Accuracy: A Hybrid MP2:DFT Study. *J. Am. Chem. Soc.* **2010**, *132*, 11525–11538.

(74) Tranca, I.; Smerieri, M.; Savio, L.; Vattuone, L.; Costa, D.; Tielens, F. Unraveling the Self-Assembly of the (S)-Glutamic Acid “Flower” Structure on Ag(100). *Langmuir* **2013**, *29*, 7876–7884.

(75) Lo, C. S.; Radhakrishnan, R.; Trout, B. L. Application of Transition Path Sampling Methods in Catalysis: A new Mechanism for C–C Bond Formation in the Methanol Coupling Reaction in Chabazite. *Catal. Today* **2005**, *105*, 93–105.

(76) Chandler, D., Berne, B. J., Ciccotti, G., Coker, D. F., Eds.; *Classical and Quantum Dynamics in Condensed Phase Simulations*; World Scientific: Singapore, 1998, 51–66.

(77) Dellago, C.; Bolhuis, P. G.; Csajka, F. S.; Chandler, D. Transition Path Sampling and the Calculation of Rate Constants. *J. Chem. Phys.* **1998**, *108*, 1964–1977.

(78) Dellago, C.; Bolhuis, P. G.; Chandler, D. Efficient Transition Path Sampling: Application to Lennard-Jones Cluster Rearrangements. *J. Chem. Phys.* **1998**, *108*, 9236–9245.

- (79) Bolhuis, P. G.; Dellago, C.; Chandler, D. Sampling Ensembles of Deterministic Transition Pathways. *Faraday Discuss.* **1998**, *110*, 421–436.
- (80) Dellago, C.; Bolhuis, P. G.; Chandler, D. On the Calculation of Reaction Rate Constants in the Transition Path Ensemble. *J. Chem. Phys.* **1999**, *110*, 6617–6625.
- (81) Bolhuis, P. G.; Dellago, C.; Chandler, D. Reaction Coordinates of Biomolecular Isomerization. *Proc. Natl. Acad. Sci. U.S.A.* **2000**, *97*, 5877–5882.
- (82) Dellago, C.; Bolhuis, P. G.; Geissler, P. L. *Transition Path Sampling*; Advances in Chemical Physics, Vol. 123; John Wiley & Sons: Hoboken, NJ, 2002; pp 1–78.
- (83) Bolhuis, P. G.; Dellago, C.; Chandler, D.; Geissler, P. L. Transition Path Sampling: Throwing Ropes Over Rough Mountain Passes, in the Dark. *Annu. Rev. Phys. Chem.* **2002**, *53*, 291–318.
- (84) Weinan, E.; Vanden-Eijnden, E. Transition-Path Theory and Path-Finding Algorithms for the Study of Rare Events. *Annu. Rev. Phys. Chem.* **2010**, *61*, 391–420.
- (85) Dobler, J.; Pritzsche, M.; Sauer, J. Oxidation of Methanol to Formaldehyde on Supported Vanadium Oxide Catalysts Compared to Gas Phase Molecules. *J. Am. Chem. Soc.* **2005**, *127*, 10861–10868.
- (86) Romanyshyn, Y.; Guimond, S.; Kuhlbeck, H.; Kaya, S.; Blum, R. P.; Niehus, H.; Shaikhutdinov, S.; Simic-Milosevic, V.; Nilius, N.; Freund, H. J.; Ganduglia-Pirovano, M. V.; Fortrie, R.; Dobler, J.; Sauer, J. Selectivity in Methanol Oxidation as Studied on Model Systems Involving Vanadium Oxides. *Top. Catal.* **2008**, *50*, 106–115.
- (87) Blaszkowski, S. R.; Van Santen, R. A. Density Functional Theory Calculations of the Activation of Methanol by a Brønsted Zeolitic Proton. *J. Phys. Chem.* **1995**, *99*, 11728–11738.
- (88) Zicovich-Wilson, C. M.; Viruela, P.; Corma, A. Formation of Surface Methoxy Groups on H-Zeolites from Methanol. A Quantum Chemical Study. *J. Phys. Chem.* **1995**, *99*, 13224–13231.
- (89) Sinclair, P. E.; Catlow, C. R. A. Density Functional Theory Calculations of Adsorption and Reactivity of Methanol at Alumino-Silicate Brønsted Acid Centers. *J. Chem. Soc. Faraday Trans.* **1997**, *93*, 333–345.
- (90) Govind, N.; Andzelm, J.; Reindel, K.; Gitzgerald, G. Zeolite-Catalyzed Hydrocarbon Formation from Methanol: Density Functional Simulations. *Int. J. Mol. Sci.* **2002**, *3*, 423–434.
- (91) Dzwigaj, S.; Peltre, M. J.; Massiani, P.; Davidson, A.; Che, M.; Sen, T.; Sivasanker, S. Incorporation of Vanadium Species in a Dealuminated  $\beta$  Zeolite. *Chem. Commun.* **1998**, 87–88.
- (92) Dzwigaj, S.; Massiani, P.; Davidson, A.; Che, M. Role of Silanol Groups in the Incorporation of V in  $\beta$  Zeolite. *J. Mol. Catal. A* **2000**, *155*, 169–182.
- (93) Soda, R. Infrared Absorption Spectra of Quartz and Some Other Silica Modification. *Bull. Chem. Soc. Jpn.* **1961**, *34*, 1491–1495.
- (94) Duran, A.; Serna, C.; Fornes, V.; Fernandez-Navarro, J. M. Structural Considerations about SiO<sub>2</sub> Glasses Prepared by Sol-Gel. *J. Non-Cryst. Solids* **1986**, *82*, 69–77.
- (95) Hajjar, R.; Millot, Y.; Man, P. P.; Che, M.; Dzwigaj, S. Two Kinds of Framework Al Sites Studied in BEA Zeolite by X-Ray Diffraction, Fourier Transform Infrared Spectroscopy, NMR Techniques and V Probe. *J. Phys. Chem. C* **2008**, *112*, 20167–20175.
- (96) Tatibouët, J. M. Methanol Oxidation as a Catalytic Surface Probe. *Appl. Catal., A* **1997**, *148*, 213–252.
- (97) Busca, G.; Elmi, A. S.; Forzatti, P. Mechanism of Selective Methanol Oxidation over Vanadium Oxide-Titanium Oxide Catalysts: a FT-IR and Flow Reactor Study. *J. Phys. Chem.* **1987**, *91*, 5263–5269.